THE JOURNAL OF PHYSICAL CHEMISTRY A

Article

pubs.acs.org/JPCA

Evolution of Silver Nanoparticles in the Rat Lung Investigated by X-ray Absorption Spectroscopy

R. Andrew Davidson,[†] Donald S. Anderson,[‡] Laura S. Van Winkle,[‡] Kent E. Pinkerton,[‡] and T. Guo*[,†]

[†]Department of Chemistry and [‡]Center for Health and the Environment, University of California, Davis, California 95616, United States

Supporting Information

ABSTRACT: Following a 6-h inhalation exposure to aerosolized 20 and 110 nm diameter silver nanoparticles, lung tissues from rats were investigated with X-ray absorption spectroscopy, which can identify the chemical state of silver species. Lung tissues were processed immediately after sacrifice of the animals at 0, 1, 3, and 7 days post exposure and the samples were stored in an inert and low-temperature environment until measured. We found that it is critical to follow a proper processing, storage and measurement protocol; otherwise only silver oxides are detected after inhalation even for the larger nanoparticles. The results of X-ray absorption spectroscopy measurements taken in air at 85 K suggest that the dominating silver species in all the postexposure lung tissues were metallic silver, not silver oxide, or solvated silver cations. The results further indicate that the silver nanoparticles in the tissues were transformed from the original nanoparticles to other forms of metallic silver nanomaterials and the rate of this transformation depended on the size of the original nanoparticles. We found that 20 nm diameter silver nanoparticles were significantly modified after aerosolization and 6-h inhalation/deposition, whereas larger, 110 nm diameter nanoparticles were largely unchanged. Over the seven-day postexposure period the smaller 20 nm silver nanoparticles underwent less change in the lung tissue than the larger 110 nm silver nanoparticles. In contrast, silica-coated gold nanoparticles did not undergo any modification processes and remained as the initial nanoparticles throughout the 7-day study period.

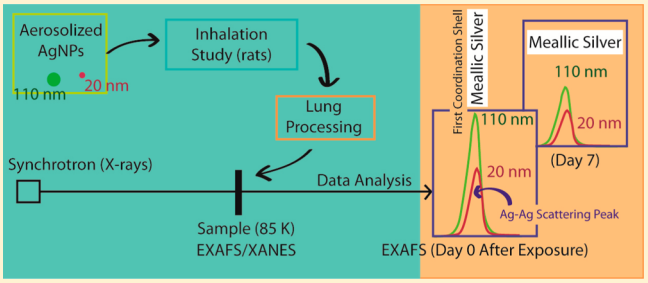

INTRODUCTION

Engineered nanomaterials (ENMs), such as silver nanoparticles (AgNPs), have been used in many existing technologies and may impact many future applications.[1] For example, AgNPs are being explored in inhalation therapy for respiratory infections and allergic airway inflammation because of their potent antimicrobial properties.[2−5] These ENMs will eventually end up in the environment, and human exposure by multiple routes, including inhalation, is likely.[6] For example, pulmonary exposure to AgNPs can occur during manufacturing. Another possible exposure is to aerosol sprays or via inhalation of water droplets containing AgNPs.[7] The toxicity of AgNPs that is responsible for their medicinal use has been investigated,[8−21] which is attributed to the toxicity of Ag^+ ions in aqueous solution, a species that possess antimicrobial properties and is found to react with various biomolecules.[22−29] Given that AgNPs can enter the lungs through inhalation and AgNPs may be potentially toxic, it is important to know the impact of ENMs such as AgNPs on the human body but especially the lung, where they will likely deposit when inhaled.

The determination of the actual Ag species in the lungs at different stages following deposition is important for understanding the origin of toxicity for AgNPs. Unlike other more stable nanomaterials such as gold nanoparticles, AgNPs may be significantly modified in the body and especially in the lungs, which are both an oxidizing and reducing environment.[30−33] Lability of AgNPs has been extensively demonstrated. For example, AgNPs dissolve in water at different pH and in the cellular and biological environment to form Ag ions.[21,34−36] These ions may undergo various transformations in different chemical environments. For instance, Ag^+ ions can be reduced to form small nanoparticles in pants or other environments.[37,38] It is also known that Ag in Au/Ag core−shell nanostructures (~80 nm in diameter) dissolve in water under X-ray irradiation and much smaller (<5 nm) AgNPs are formed. The dissolved Ag ions are chemically reduced by species available in solution, such as solvated electrons generated in water under X-ray irradiation. This again suggests that large AgNPs can dissolve and reform into smaller AgNPs in a redox environment.[39] On the basis of these findings, it is entirely possible that AgNPs may be partially or completely modified and continue to change in the lungs, and it is critical to identify and track transient Ag species in the lungs as a means to determine their eventual fate and understand those factors that may contribute to toxic effects.

Received: October 6, 2014
Revised: November 25, 2014
Published: December 16, 2014

DOI: 10.1021/jp510103m
J. Phys. Chem. A 2015, 119, 281−289

Several analytical methods can characterize the physicochemical properties of nanomaterials in the lungs, although each has its own shortcomings. Inductively coupled plasma−mass spectrometry (ICP-MS) and recent work using autometallography can help locate small amounts of Ag in the lungs.[21,40] However, critical chemical information such as oxidation state and whether the original AgNPs stay intact or are dissolved and reduced to form smaller AgNPs cannot be revealed using these methods. Traditional centrifuge separation in combination with atomic absorption spectroscopy cannot conclusively assign the chemical state of Ag species because small (∼1 nm diameter) Ag neutral nanoparticles may stay in the supernatant after centrifugation, even at 13 000 rpm or filtered with membranes.[41,42] X-ray photoelectron spectroscopy (XPS) may be used to identify the chemical state of the nanomaterials and their derivatives.[43] However, sample preparation is difficult and strict measurement conditions are required. In addition, the sample size is extremely small because XPS is a surface probe approach, so only a small portion of the sample is probed. Electron microscopy, such as transmission electron microscopy (TEM), may be difficult to employ to study the chemical state of ENMs in the environment and body because of the limitation of being able to only perform basic elemental analysis.[44] As a result, none of the reported methods can detect the needed physicochemical properties of Ag species in the lungs, information that is key to understanding the observed biological responses to AgNPs.

X-ray absorption spectroscopy (XAS) is a powerful method to study the properties of ENMs in biological systems including the lungs.[45] XAS is equivalent to a local electron diffraction method that can probe the chemical environment or local, short-range order around a specific X-ray absorbing element, which can be Ag if AgNPs are under investigation. XAS can determine at least two critical chemical parameters: chemical shift and local bonding environment. These parameters can help reveal the dominant transient Ag species. The first parameter can be used to determine the oxidation state of the element under investigation. The second can be used to infer the size or surface area of nanoparticles and whether Ag species are in metallic nanoparticles, oxide nanoparticles or dissolved in water. The sensitivity of XAS is high, down to micrograms of Ag in grams of tissues, suitable for detecting AgNPs in lung tissues under inhalation conditions. In addition, X-rays are highly penetrating, capable of studying most elements including Ag and Au in mm thick samples. To date, XAS has been used to study silver nanomaterials (AgNMs) in several different background materials,[46−50] predominantly at room temperature and seldom at low temperatures.[49,51] Hence XAS is a promising method to determine chemical information on the Ag species in the lungs.

One challenge for performing XAS measurements is that those experiments are generally conducted at national facilities and it is critical to minimize changes occurring to ENMs in lung tissues retrieved after an in vivo, preferably inhalation, exposure. These exposures are often conducted at specialized facilities far from the site of eventual analysis. Because lung tissues are full of oxidative and reducing agents, even after the animals are sacrificed, Ag species may continuously change chemically until XAS measurements are conducted. As a result, the samples and experimental protocols have to be designed to eliminate further evolution of the transient Ag species.

Here we present the outcome of the first attempt to use XAS to characterize Ag species in rat lungs after inhalation exposure of aerosolized AgNPs. In the following, the methods and results are presented, followed by discussion of the results. We have found that XAS can, in principle, be used to retrieve important chemical information on the Ag species in the lungs from animals that have undergone practical exposure scenarios, such as inhalation of aerosolized ENMs. Through this study, we have established proper protocols to employ XAS to study ENMs in rat lungs after inhalation and have obtained results that may help shed light on the mechanisms of transport and fate of AgNPs in the lungs. The current work focuses on the study of evolution of AgNPs in the lungs after deposition.

MATERIALS AND METHODS

Materials. AgNPs were manufactured by nanoComposix, Inc. (San Diego, CA), and were supplied by the National Institute of Environmental Health Sciences Centers for Nanotechnology Health Implications Research (NCNHIR) consortium. AgNPs were 20 and 110 nm in diameter and stabilized with a citrate coating. AgNPs were at a concentration of 1 mg/mL in 2 mM citrate aqueous solution and were stored in the dark at 4 °C.

AuNPs@SiO_2 Synthesis. 88 nm diameter gold nanoparticles (AuNP) cores were synthesized in a seed growth method modified from an established protocol.[52] First, a gold seed solution was made by citrate reduction.[53] Then 50 μL of $HAuCl_4$ was added to 150 mL of MilliQ (MQ) water. Once at reflux and with vigorous stirring, 6 mL of 1 wt % sodium citrate was injected rapidly. The solution was refluxed for 15 min and then allowed to cool to room temperature. Seed growth was performed in three sequential growth steps. 0.3 g of poly(vinylpyrrolidone) (PVP) in 10 mL of MQ water was added to the final solution. The PVP coating proceeded overnight. Excess PVP was removed by centrifuging at 5.5k rpm for 15 min. Centrifugation and washing was performed twice and the AuNPs resuspended into 5 mL of MQ water. The 5 mL of AuNPs was added to 37.5 mL of ethanol and 0.5 mL of 28 wt % NH_3OH. With stirring, we added 0.5 mL of tetraethyl orthosilicate (TEOS), and the reaction proceeded overnight. The solution was purified by centrifuging and washing with 40 mL of MQ water five times. AuNPs@SiO_2 samples were collected.

Aerosolization of AgNPs and Inhalation. AgNPs were aerosolized using a BGI 6-jet Collison nebulizer to produce liquid aerosol droplets. The droplets were dehydrated using two TSI diffusion dryers (3062, TSI) and charge was neutralized using a Krypton-85 β-particle source prior to delivery to the nose-only exposure unit.[54,55] Excess particles were scavenged from the exposure unit into a filter using a vacuum pump. Particle mass concentration was determined using gravimetric analysis of filters and particle number concentration using a scanning mobility particle scanner (SMPS, 3071/3010, TSI), which was also used to measure the aerosol size.

Lung Sample Preparation. Twelve week old male Sprague−Dawley rats were obtained from Harlan Laboratories and acclimated 1 week prior to exposure. Rats were housed in two per cage and provided Laboratory Rodent Diet (Purina Mills, St Louis, MO) and water ad libitum. All animal experiments were performed under protocols approved by the University of California Davis IACUC in accordance with National Institutes of Health guidelines. Rats were conditioned to the exposure tubes in the week prior to exposure by being housed in tubes for progressively longer periods of time. Rats

DOI: 10.1021/jp510103m
J. Phys. Chem. A 2015, 119, 281−289

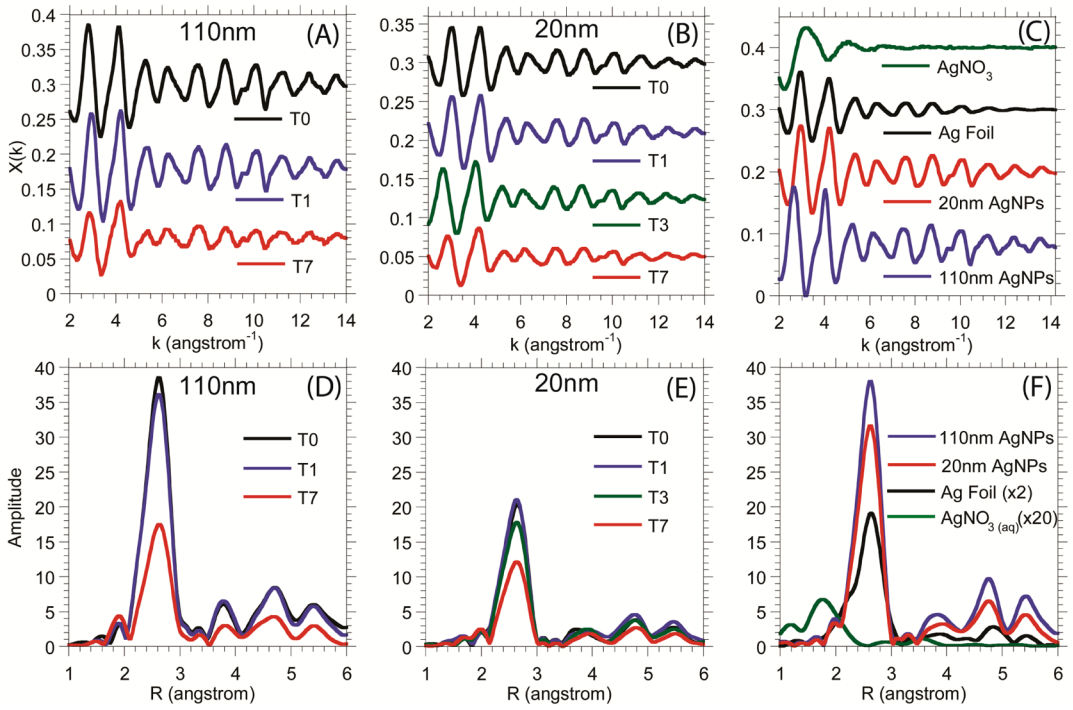

Figure 1. EXAFS results in reciprocal (A–C) and real (D–F) space. The samples include 110 nm (A/D) and 20 nm (B/E) AgNPs and several reference samples (C/F). Figure D and F are the FT counterparts of the plots shown in panels A and C, respectively. The EXAFS data are displaced vertically for visual clarity.

were exposed once to an aerosol of 20 or 110 nm AgNPs for 6 h. Animals were euthanized at the end of exposure (T0), or at 1 (T1), 3 (for 20 nm AuNPs only, T3), and 7 days (T7) post exposure using Beuthanasia-D at 7.5 mL/kg and exsanquination. The abdominal and thoracic cavities were opened, the trachea cannulated and the lung was removed en block. The lung was immediately filled with helium at 30 cm water pressure and frozen in 2-methylbutane over liquid nitrogen. A 1.0–1.5 mm section was cut from of the center of the left lobe, secured between two layers of clear adhesive tape and stored at −80 °C in an argon purged storage box.

XAS Data Collection and Processing. XAS, which includes both extended X-ray absorption fine structure (EXAFS) and X-ray absorption near edge spectroscopy (XANES), was employed to determine the oxidation state and local chemical structure of the Ag species in the lung. Both methods are useful in revealing the chemical state of the element of interest.[56,57] The patterns of XANES of the samples and different standards are often adequate to directly reveal the chemical state of the element of interest. EXAFS requires simulation but often providing more detailed structural information on the elements of interest.

The XAS experiments were conducted at beamline 7–3 at the Stanford Synchrotron Radiation Lightsource (SSRL). The beamline (Si (220) monochromator) was optimized to detect X-ray fluorescence of Ag or Au in the samples, while reducing the scattering from the soft tissues and ice in the background. Data collection was performed either at room temperature or at 85 K. For measurements performed at 85 K, the immediately frozen and inertly stored lung samples were cooled to 85 K using a liquid helium thermal station. EXAFS data (K edge of Ag and L edge of Au) were measured using a multiple element Ge detector, and each sample took more than 6 h to measure. The signals from all the detector elements were summed to obtain the EXAFS raw data. The background in the raw data was removed and the EXAFS oscillation was obtained. EXAFS data was processed using SIXPack.[58] The k range data was selected, deglitched, and then Fourier transformed (FT) to the real space. Interatomic distances (R), coordination numbers (N), and disorders (Debye–Waller factor or σ) were then optimized to fit the EXAFS data in the k space. Standard deviation of the fitting parameter is estimated by changing the parameter to double the fitting error. XANES spectra were processed similarly, although no FT was used and no fitting was performed. As a control, lung samples were also prepared and stored at room temperature without the inert environment and measured at room temperature as well. The XAS data was processed similarly as described above.

In analyzing EXAFS data, we selected EXAFS in the energy space from 25565 to 26050 eV for Ag measurements, corresponding to k reciprocal space of 2–14 Å^{-1}, which is broader than commonly used in the literature to retrieve AgNP structural information in environmental samples.[46,51] Generally speaking, the broader the k data range, the higher quality of EXAFS data. The broader range used here is enabled by low temperature (85 K) measurements and hence provides more accurate EXAFS data and higher quality fittings.

Oxidation state (os) information was retrieved by examining the chemical shift obtained from XANES data. Second derivative was taken against each XANES trace, and chemical shift (CS) of the samples was calibrated against the same internal reference of a thin silver foil at room temperature for each measured sample. For data with large noise at the inflection point, analytical formulas were created to fit the first derivative near the inflection point and then the shifts of the XANES patterns were determined. Oxidation state can be calculated by comparing the chemical shift of the samples to

DOI: 10.1021/jp510103m
J. Phys. Chem. A 2015, 119, 281–289

Table 1. Fitting Parameters of the Average Coordination Number (N), Interatomic Distance or Bond Length (R), and Debye–Waller Factor (σ) for the Ag Species in the Lung Samples Whose Results Shown in Figure 1[a]

	Ag–Ag (2.880 Å), Ag–O (2.200 Å) and Ag–Cl (2.700 Å) peak fittings (EXAFS)			
	N	R (Å)	σ (Å^2)	CS (eV) (XANES)
110 nm AgNP	9.19 ± 0.682	2.887 ± 0.003	0.00339 ± 0.0003	−0.4
lung T0 110 nm	10.11 ± 1.27	2.887 ± 0.005	0.00340 ± 0.0006	0.0
lung T1 110 nm	10.09 ± 1.16	2.886 ± 0.004	0.00364 ± 0.0005	+0.4
lung T7 110 nm	4.87 ± 0.691	2.888 ± 0.005	0.00367 ± 0.0006	+0.6
110 nm AgNP + O_2	10.08 ± 0.968	2.886 ± 0.004	0.00381 ± 0.0004	0.0
110 nm AgNP in ALF	8.63 ± 0.696	2.884 ± 0.003	0.00371 ± 0.0004	0.0
20 nm AgNP	8.58 ± 0.444	2.863 ± 0.002	0.00367 ± 0.0002	−1.4
lung T0 20 nm	5.69 ± 0.283	2.877 ± 0.002	0.00381 ± 0.0002	−2.3
lung T1 20 nm	5.75 ± 0.182	2.876 ± 0.001	0.00366 ± 0.0001	−2.9
lung T3 20 nm	5.01 ± 0.305	2.876 ± 0.002	0.00375 ± 0.0003	−2.1
lung T7 20 nm	3.50 ± 0.244	2.879 ± 0.003	0.00390 ± 0.0003	−2.0
Ag foil	7.15 ± 0.281	2.863 ± 0.002	0.00902 ± 0.0002	0.0
20 nm AgNP + O_2	8.37 ± 0.424	2.875 ± 0.002	0.00361 ± 0.0002	−1.5
$AgNO_3$ (Ag–O)	3.63 ± 3.48	1.989 ± 0.111	0.0158 ± 0.020	+2.4
$AgNO_3$ in ALF (Ag–Cl)	4.46 ± 0.371	2.634 ± 0.006	0.00755 ± 0.0009	−2.2

[a]Chemical shift (CS) values are obtained from XANES measurements described.

that of Ag foil (os = 0.0) and $AgNO_3$ (os = +1.0). No error was assigned to the CS or os.

RESULTS

EXAFS data can directly reveal the nature of chemical bonding environment through the examination of the position and the amplitude of the peaks in EXAFS data for the dominating Ag species in the lungs. Figure 1A and B show the EXAFS data in the reciprocal space obtained at 85 K of the frozen and properly stored lungs tissues exposed to 20 and 110 nm AgNPs at 0, 1, 3 (only for 20 nm), and 7 days. Figure 1D and E show the same EXAFS results after FT into the real space. In the results shown here (Figure 1D and E) there is only one dominant peak between 1 and 3 Å in the real space for all seven samples (T0, T1, T3, and T7). This peak corresponds to first Ag–Ag coordination shell around the X-ray absorbing Ag or direct Ag–Ag bonds in these samples. Other peaks at greater distances represent higher-order coordination shells around the absorbing Ag. There is little or no Ag–O peak. On the basis of this information, we conclude that Ag species in all seven samples are dominated by pristine metallic Ag. This is the first direct evidence that Ag species carried into the lungs are metallic, not oxides or sulfides, over an extensive period of time.

The amplitude of the peaks in the EXAFS data reveals how the coordination number changes over time. Results shown in Figure 1 display that the differences between EXAFS data for 20 and 110 nm AgNPs. For 110 nm AgNPs in the lungs as shown in Figure 1D, Ag in T1 samples has a slightly lower amplitude than that of Ag species in T0 samples. In contrast, amplitude for T7 is less than half of that for T0 and T1 samples. The decrease in the modulation amplitude for T7 sample is also obvious in the energy space, as shown in Figure 1A. For samples obtained with 20 nm AgNPs starting material (Figure 1E), on the other hand, the trend is similar but with two major differences. The similarity is that there is little Ag–O/N/Cl/S scattering and the main peak corresponds to Ag–Ag scattering. The differences are (1) the amplitude of the EXAFS peak of T0 for 20 nm AgNPs is significantly lower than those of 110 nm AgNPs at similar time points and (2) the change from day 0 to day 7 is less significant for Ag obtained with 20 nm AgNPs than 110 nm AgNPs. These observations seem to agree with the recently obtained inhalation toxicity data.[40] From these data, it is evident that 20 nm AgNPs were modified more significantly at the onset of deposition, but followed by smaller changes over the 7-day period than 110 nm AgNPs.

Several silver references or standards, including a metallic Ag foil, 20 and 110 nm AgNPs and frozen Ag nitrate aqueous solution were measured, and their results are shown in Figure 1C and F. Ag foil was the only sample that was measured at room temperature while the rest were all measured at 85 K. EXAFS results for T0 of 110 nm shown in Figure 1A and D are similar to the pristine 110 nm AgNPs, but T0 data for 20 nm is quite different from that of 20 nm pristine AgNPs: The 20 nm T0 sample has a much lower EXAFS peak corresponding to Ag–Ag scattering. Both 20 and 110 nm pristine AgNPs in water are barely oxidized, as shown in Figure 1C and F, and they are close to the pristine AgNPs. In contrast, there is no Ag–Ag peak in Ag nitrate; only Ag–O or Ag–N bond appears in frozen $AgNO_3$ aqueous solution. The $AgNO_3$ data in the R space is obtained from the k space EXAFS data with slightly a smaller range of k space data of 2–9 Å^{-1} because of the lack of oscillation beyond this range, especially in the high k region. A single peak corresponding to Ag–O is found from our measurements. This peak is more difficult to observe if the sample is measured at room temperature because of greater disorder. The measured results of these references suggest that the inhaled 20 and 110 nm AgNPs and their derivatives remain metallic in rat lungs after 7 days, albeit the nanoparticles of two sizes behaved differently.

We also measured $AgNO_3$ and 110 nm AgNPs incubated in artificial lung fluids (ALF) as well as 20 and 110 nm AgNPs in O_2 bubbled water. The results are shown in Supporting Information Figure SI-1. AgNPs in O_2 bubbled water did not change significantly compared with pristine AgNPs. For $AgNO_3$ in ALF, there was clearly white precipitate and the EXAFS results in the real space show only the Ag–Cl peak; neither Ag–O nor Ag–Ag peak exists. The source of Cl is most likely from high salt concentration in ALF. Only AgCl precipitates formed because of presence of Cl ions in ALF. Amplitude of the main EXAFS peak for Ag in 110 nm AgNPs in ALF sample is slightly lower than pristine AgNPs, implying that ALF could do the same to AgNPs as the lungs did to the AgNPs. It is

DOI: 10.1021/jp510103m
J. Phys. Chem. A 2015, 119, 281–289

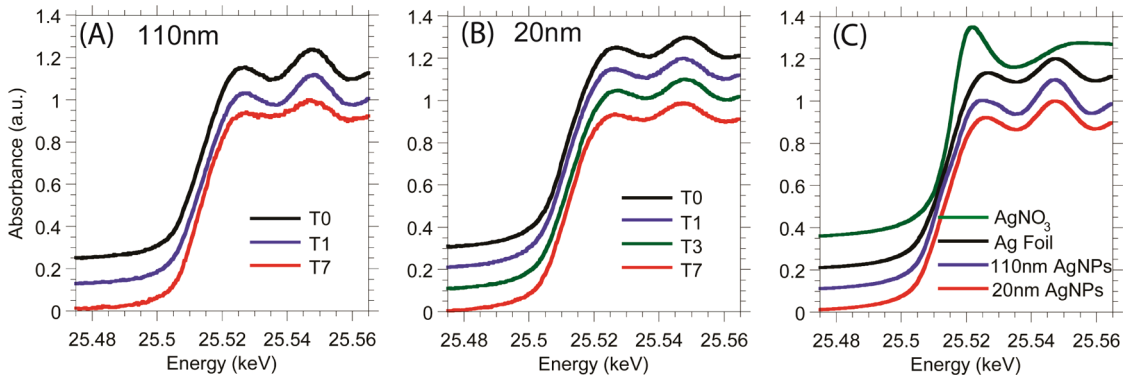

Figure 2. XANES results of the inhaled 110 and 20 nm AgNPs and references samples.

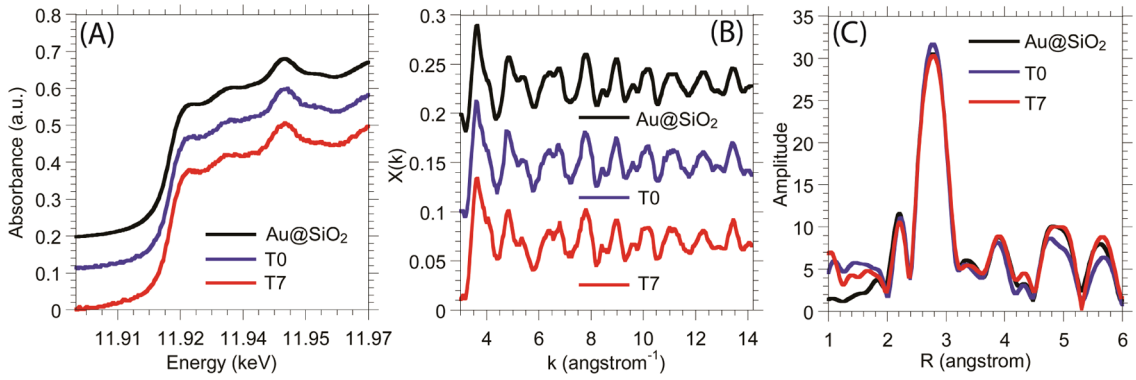

Figure 3. XANES (A) and EXAFS (B/C) data for the AuNPs@SiO_2. There is only one EXAFS peak in the real space in the direct bonding region of 1−3 Å. The changes over 7 days among the samples studied were minimal.

worth pointing out that AgNPs were only incubated in ALF for a few hours, possibly explaining the relatively small decrease in amplitude of EXAFS signal in the R space shown in Supporting Information Figure SI-1C.

Table 1 lists the fitted parameters of R (distance between two scatters), Debye−Waller factors (disorder or σ) and coordination numbers N of the lung samples studied here and shown in Figure 1. In fitting, the most intense peak between 1.0 and 3.0 Å corresponding to either Ag−Ag or Ag−O was isolated and selected and then fitted to the selected data in a chosen k range in the reciprocal space. The fitting is straightforward because of the dominant peak for most of the samples. An example of the peak isolation and fitting is shown in Supporting Information Figure SI-2. This peak from each sample is fit independently. Fitting results for $AgNO_3$ samples are also listed.

On the basis of Table 1, it is clear that the two types of AgNPs continue to change in the lungs after inhalation/deposition. For 110 nm, there is no initial drop from pristine to day 0 followed by a significant drop of 52% from T0/T1 of 10.0 ± 1.2 to day 7 of 4.87 ± 0.70. Pristine 110 nm AgNPs and T0 Ag species have similar disorders, and *N* for the pristine AgNPs (9.2 ± 0.7) and T0/T1 are within statistical errors. In contrast, 20 nm AgNPs behaved differently from the 110 nm AgNPs. The average N for 20 nm before inhalation is 8.6 ± 0.4, with a similar disorder to T0 sample. Immediately after inhalation, the N of Ag in the lungs at T1 drops to 5.8 ± 0.19, a 33% drop that may be caused by either the inhalation process or how rat lungs take up these smaller nanoparticles. The N then only decreases further down to 3.50 ± 0.24, another 39% drop over the next 7 days. Supporting Information Figure SI-3 summarizes the results.

The disorder varies only slightly among these Ag species measured at 85 K. The disorder is slightly less for the pristine 110 nm AgNPs and Ag species in T0 sample. However, Ag species in the lungs derived from 110 nm AgNPs in T7 sample have a similar disorder even these Ag species have a much lower average N than the pristine AgNPs. The disorders of other AgNPs measured at 85 K are similar, staying within ±7% of the average value of 0.00365 $Å^2$. The disorder for Ag foil, the only sample measured at room temperature, is almost three times that of other samples measured at 85 K and is very close to the previous reported values.[59] Disorder for $AgNO_3$ is much higher, due to the randomness in distance between Ag cations and nearby oxygen or nitrogen in solution.

In addition to EXAFS measurements, XANES can more directly detect small changes to the oxidation state of the Ag species in the samples through the measurement of chemical shift. The XANES results of the samples studied above are shown in Figure 2. On the basis of Figure 2A, it is evident that day 7 sample of 110 nm AgNPs has a smaller modulation amplitude than that of day 0 or 1 sample in the XANES region. The raw data showed the modulation amplitude in T7 XANES data was about 50% of that T0 and T1, agreeing with the EXAFS data. On the other hand, the decrease from T0 to T7 is less for 20 nm samples.

The chemical shifts, which are represented by the inflection points or the shifts of the first derivative patterns of the XANES data, are listed in Table 1. The two benchmark samples are bulk Ag foil and $AgNO_3$, and the chemical shifts for these two samples are 0.0 and +2.4 eV. It is clear that nitrate has a much greater chemical shift than Ag foil in which Ag species should be neutral. Ag species in 110 nm T0 sample and two other 110

DOI: 10.1021/jp510103m
J. Phys. Chem. A 2015, 119, 281−289

nm AgNP control samples that are exposed to O_2 and ALF have approximately no charge. There are small amounts of positive charge on Ag in the 110 nm T1 and T7 samples, agreeing with the EXAFS data showing no Ag−O peak. In contrast, all of the 20 nm AgNP samples including the pristine 20 nm AgNPs seem to have negative charge on them, meaning that the Ag species are chemically reduced instead of oxidized.

As a control, we also investigated silica-coated gold nanoparticles (AuNPs@SiO_2). Because of the protection layer of 20-nm thick SiO_2, we did not expect this nanomaterial be modified in the lungs. The results of AuNPs@SiO_2 at T0 and T7 day are shown in Figure 3. The background scattering from ice/tissue is stronger due to the lower energy of X-rays used to study the L edge of Au at approximately 13 keV. XANES data shown in Figure 3A reveals no oxidation. From the EXAFS data, which is shown in Figure 3B/C, it is also clear that no oxidation occurred. It is important to note that the EXAFS data of AuNPs@SiO_2 in T0 and T7 samples are almost identical, without much change to N, which is in contrast to those of AgNPs shown in Figure 1D/E. It indicates that AuNPs were largely the same after spending 7 days in the lungs, while AgNPs underwent measurable transformations.

The sample preparation and measurement protocols are critical to the success of the measurements. If not immediately frozen and stored in the inert environment and measured at low temperatures, the XAS results are invalid. The data of these samples taken at room temperature is shown in Supporting Information Figure SI-4. In contrast to immediately freezing/storage in the inert environment, AgNPs stored exposed to air and measured at room temperature were completely oxidized and possibly dissolved. Supporting Information Figure SI-4A shows the XANES results of these samples without immediate freezing and storage in inert environment. Ag species of even 110 nm AgNPs in the lungs are mostly oxidized, similar to that in $AgNO_3$ (aq). Supporting Information Figure SI-4B and C show the EXAFS results in the k and R space of the lung samples without immediate freezing and storage in the inert environment. It is clear that the quality of the data is poor in the high k region, because of the much larger Debye−Waller factors or disorder of the species under investigation at room temperature. For 110 nm AgNPs, the peaks at the left of the main peak became more prominent and the peak intensities increase further for O_2 bubbled AgNPs. In contrast, for 110 nm AgNPs in the lungs, whether it is after 1 or 7 days, the Ag−Ag peak largely disappeared, similar to that in the standard $AgNO_3$ (aq). These results suggest that if the samples were not properly prepared and stored, 110 nm AgNPs were completely oxidized or even dissolved in the lungs after just 1 day because of the extensive time of several weeks between the sample preparation and XAS measurements. On the other hand, Ag species still possess Ag−Ag scattering after O_2 bubbling through the AgNPs solution (aq) for 24 h. The results shown here demonstrate the importance of properly treating and measuring the samples in order to preserve the chemical state of Ag species in lung tissues obtained post exposure.

DISCUSSION

The absorption changes shown in XANES raw data (not shown) can be used to infer the amount of Ag in the samples, which shows approximately the same amounts of Ag in all the lungs at T0. These results are corroborated by an ICP-MS study of the total amounts of Ag in the lung, which were 321 and 357 ng at T0 for 20 and 110 nm AgNPs following inhalation.[55] This shows that even small amounts of Ag species deposited in the lung can be studied with XAS measurements to reveal their chemical structures.

We did not investigate the effect of aerosolization and inhalation process on the modification of AgNPs, which may cause temporary aggregation to some AgNPs. We do not believe that the aerosolization process alters the chemical state of the Ag species in AgNPs. For 110 nm AgNPs, there was little or no aggregation—the SMPS measurements suggested the size of 110 nm.[55] For 20 nm AgNPs, the SMPS measurements showed the size of 77 nm, which may be caused by aggregation, as well as by sodium citrate salt in the solution. Because the nebulizer produces droplets with a mass medium diameter of 1.9 μm, each liquid droplet may contain single (110 nm AgNP) or multiple (20 nm AgNPs) AgNPs. Upon drying, the final product may contain either single AgNPs or aggregates of several AgNPs. In the presence of citrate, such aggregation generates little chemical modification to the Ag species in the nanoparticles and once these nanoparticles are deposited on the surface in the lung, they should behave similarly as individual citrate-covered AgNPs.

It is interesting to note that the values of the average coordination number N are small (around 3.5 to 5.5) for the Ag species detected at the end of 7-day postexposure. These values correspond to the N values for 3 and 6 nm diameter AgNPs reported in the literature.[51] For perfect crystalline Ag bulk, the value of N should be close to 12.[51] The value of N decreases as the particle size reduces or surface area increases because there are more surface atoms. Surface atoms in a 111 facet of a face-center-cube crystalline structure have fewer than 9 neighbors whereas the bulk atoms have 12. The atoms at the edges have even fewer neighbors. However, even for a 100-atom nanoparticle corresponding to a roughly 1.0 nm diameter nanoparticle, the average N of the first coordination shell is approximated 8.0 if the cluster is perfectly crystalline or cuboctahedral.[60,61] The low N measured here, and those shown in the literature for small AgNPs, seems to suggest that these Ag species may be contained in either very small AgNPs, of the order 1 nm in diameter, or in highly porous larger sized (3−6 nm or even larger) Ag nanomaterials, possibly resembling Ag-doped zeolites.[49] This means that the Ag species in T7 may contain a large portion of such new metallic Ag species that are derived from the original 20 or 110 nm AgNPs.

The dominant metallic Ag species detected in the lungs suggests that if Ag^+ ions are responsible for the observed toxicity, then those ions must be short-lived and be readily reduced to neutral atoms chemically, which may form small AgNPs. The fact that Ag−Ag scattering accounts for the only major peak in EXAFS suggests that majority of Ag species in the lungs at any time are in the form of small metallic nanoparticles or highly porous metallic nanomaterials such as zeolites.

The results also show that Ag species in the lungs derived from 110 nm AgNPs change more quickly than 20 nm AgNPs and the inhalation process itself seems to be able to modify the smaller 20 nm AgNPs at the onset of inhalation, which does not happen for 110 nm AgNPs. This seems to be in agreement with a recent inhalation toxicity study.[40] For 20 nm AgNPs, there was more significant modification to the nanoparticles from aerosolization to inhalation/deposition. On the other hand, the change occurring to the inhaled 20 nm AgNPs over the 7 day period after deposition is less marked than in the larger 110 nm AgNPs. These findings suggest that size does play a role in

DOI: 10.1021/jp510103m
J. Phys. Chem. A 2015, 119, 281−289

determining the chemical fate of these nanomaterials in animals.

There are several possible explanations for the formation of smaller AgNPs in the T7 sample. The most plausible explanation is that the surface Ag atoms were oxidized and dissolved from the inhaled AgNPs and these dissolved atoms, or ions, then form smaller AgNPs. Because the average coordination number is only around 4.0 and because XAS is an ensemble measurement, the average surface area of Ag species in the measured volume must be large. Since the average Ag species are still metallic, it means that the AgNPs need to be broken down but the new Ag species must stay nonoxidized through chemical reduction, which is possible in the lungs. This proposed oxidation, dissolution and reformation process has been observed in the past in a redox environment.[39] We speculate that there might be temporary high concentrations of Ag^+ ions around the original AgNPs as the nanoparticles dissolve into ions that are immediately reduced to metallic Ag atoms and then reform into small AgNPs. This process continues until the AgNPs are depleted or the concentration of Ag ions/atoms becomes too low to form small nanoparticles. This way AgNPs continuously evolve until Ag species are cleared from the lungs. The second possibility is that most original large AgNPs were dissolved away and cleared from the lungs on day 7, leaving behind only the newly formed smaller AgNPs. However, in order for this scenario to be true, the signal strength of T7 sample has to be much weaker (orders of magnitude), which is not the case. The third possible scenario is that there is no dissolution of AgNPs but just that the smaller AgNPs in the original AgNPs solution were the ones that remained in the lungs after larger AgNPs were cleared from the lungs. Because larger AgNPs carry much more Ag, this scenario also requires that the absolute amount of Ag in the lungs decreases significantly at T7, which was not observed. ICP-MS measurements of the dose of AgNPs in the lungs found similar amounts of Ag species in the lungs 7 days after inhalation exposure to 20 and 110 nm AgNPs, proving that significant amounts of Ag species remain in the lungs for a prolonged period of time.[55] The fourth pathway is that AgNPs simply become more porous as they are transformed into zeolite-like nanomaterials.

The negative chemical shifts for Ag species derived from 20 nm AgNPs are uncommon since more often Ag is oxidized and possesses positive chemical shifts. However, Ag or Au nanoparticles may possess negative charges on the surface.[62] If the surface area is large to give rise to small N, it is possible that these Ag species may be negatively charged because of interaction with ligands. Because the Ag species in all samples are metallic, the negative charge on Ag species derived from 20 nm AgNPs does not show in the EXAFS data. It is intriguing that the 20 and 110 nm or derivatives in the lungs had different chemical shifts, a result that requires further scrutiny in the future.

Our results suggest that it is possible to use XAS to study inhaled AgNPs and determine the chemical state of the Ag species in the lungs after inhalation. Important steps must be taken to obtain the desired data that can be used to help elucidate the transport and fate of AgNPs in the lungs. One of the most critical procedures is that lung samples need to be immediately frozen and stored in an inert environment to ensure stoppage of the oxidation process after lung samples are taken. It is also important to take measurements at low temperatures to reduce noise at high k values and maintain a weakly oxidizing environment.

CONCLUSIONS

We used extended X-ray absorption fine structure (EXAFS) and X-ray absorption near edge spectroscopy (XANES) to study AgNPs in the lungs. The samples were prepared after inhalation of aerosolized AgNPs aqueous solution by rats and the prepared lung samples were frozen in inert environment immediately after inhalation exposure experiment. The 20 and 110 nm AgNPs in lung tissues were then measured at 85 K at SSRL. XANES data suggest that all the AgNPs in day 0, 1, 3, and 7 are metallic and AgNPs in day 7 sample were different from those at day 0 and 1. EXAFS data confirmed that the dominant Ag species in the lungs remain metallic throughout the seven-day period and the nanoparticles were possibly dissolved and smaller AgNPs or zeolite AgNMs are formed in the lungs over the seven-day period. Furthermore, the rate of change of these nanoparticles is size dependent and larger 110 nm AgNPs experienced more dramatic change over 7 day period than the smaller 20 nm particles. Because XAS is an ensemble measurement, the results shown here do not exclude the existence of small amounts of Ag atoms or ions.

ASSOCIATED CONTENT

Supporting Information

XANES and EXAFS data of several reference samples, examples of the EXAFS data processing and fitting, and change of N for the 110 and 20 nm AgNPs inhaled by the lungs. This material is available free of charge via the Internet at http://pubs.acs.org.

AUTHOR INFORMATION

Corresponding Author

*E-mail: tguo@ucdavis.edu.

Notes

The authors declare no competing financial interest.

ACKNOWLEDGMENTS

Grant support (U01 ES020127) and silver nanomaterials used in this study are procured, characterized, and provided by NIEHS Centers for Nanotechnology Health Implications Research (NCNHIR) Consortium. R.A.D. is grateful for the training in X-ray spectroscopy made possible by a National Science Foundation grant (CHE-1307529), and D.S.A. is grateful for support from a Superfund Research Program Fellowship (P42 ES04699). Use of the Stanford Synchrotron Radiation Lightsource, SLAC National Accelerator Laboratory, is supported by the U.S. Department of Energy, Office of Science, Office of Basic Energy Sciences under Contract No. DE-AC02-76SF00515

ABBREVIATIONS

ALF, artificial lung fluid; AgNPs, silver nanoparticles; AuNPs, gold nanoparticles; ENMs, engineered nanomaterials; EXAFS, extended X-ray absorption fine structure; FT, Fourier transform; ICP-MS, inductively coupled plasma−mass spectrometry; SMPS, size mobility particle scanner; TEM, transmission electron microscopy; TEOS, tetraethyl orthosilicate; XANES, X-ray absorption near-edge structure; XAS, X-ray absorption spectroscopy; XPS, X-ray photoelectron spectroscopy

DOI: 10.1021/jp510103m
J. Phys. Chem. A 2015, 119, 281−289

REFERENCES

(1) Pelgrift, R. Y.; Friedman, A. J. Nanotechnology as a Therapeutic Tool to Combat Microbial Resistance. *Adv. Drug Delivery Rev.* **2013**, *65*, 1803−1815.

(2) Hindi, K. M.; Ditto, A. J.; Panzner, M. J.; Medvetz, D. A.; Han, D. S.; Hovis, C. E.; Hilliard, J. K.; Taylor, J. B.; Yun, Y. H.; Cannon, C. L.; Youngs, W. J. The Antimicrobial Efficacy of Sustained Release Silver−Carbene Complex-Loaded L-Tyrosine Polyphosphate Nanoparticles: Characterization, in Vitro and in Vivo Studies. *Biomaterials* **2009**, *30*, 3771−3779.

(3) Jang, S.; Park, J. W.; Cha, H. R.; Jung, S. Y.; Lee, J. E.; Jung, S. S.; Kim, J. O.; Kim, S. Y.; Lee, C. S.; Park, H. S. Silver Nanoparticles Modify Vegf Signaling Pathway and Mucus Hypersecretion in Allergic Airway Inflammation. *Int. J. Nanomed.* **2012**, *7*, 1329−1343.

(4) Xiang, D. X.; Zheng, Y.; Duan, W.; Li, X.; Yin, J. J.; Shigdar, S.; O'Connor, M. L.; Marappan, M.; Zhao, X. J.; Miao, Y. Q.; Xiang, B.; Zheng, C. L. Inhibition of a/Human/Hubei/3/2005 (H3n2) Influenza Virus Infection by Silver Nanoparticles in Vitro and in Vivo. *Int. J. Nanomed.* **2013**, *8*, 4103−4113.

(5) Sondi, I.; Salopek-Sondi, B. Silver Nanoparticles as Antimicrobial Agent: A Case Study on *E. Coli* as a Model for Gram-Negative Bacteria. *J. Colloid Interface Sci.* **2004**, *275*, 177−182.

(6) Seltenrich, N. Nanosilver Weighing the Risks and Benefits. *Environ. Health Perspect.* **2013**, *121*, A220−A225.

(7) Quadros, M. E.; Marr, L. C. Environmental and Human Health Risks of Aerosolized Silver Nanoparticles. *J. Air Waste Manage. Assoc.* **2010**, *60*, 770−781.

(8) Ji, J. H.; Jung, J. H.; Kim, S. S.; Yoon, J. U.; Park, J. D.; Choi, B. S.; Chung, Y. H.; Kwon, I. H.; Jeong, J.; Han, B. S.; Shin, J. H.; Sung, J. H.; Song, K. S.; Yu, I. J. Twenty-Eight-Day Inhalation Toxicity Study of Silver Nanoparticles in Sprague-Dawley Rats. *Inhalation Toxicol.* **2007**, *19*, 857−871.

(9) Asharani, P. V.; Wu, Y. L.; Gong, Z. Y.; Valiyaveettil, S. Toxicity of Silver Nanoparticles in Zebrafish Models. *Nanotechnology* **2008**, *19*, No. 255102.

(10) Bar-Ilan, O.; Albrecht, R. M.; Fako, V. E.; Furgeson, D. Y. Toxicity Assessments of Multisized Gold and Silver Nanoparticles in Zebrafish Embryos. *Small* **2009**, *5*, 1897−1910.

(11) Kim, S.; Choi, J. E.; Choi, J.; Chung, K. H.; Park, K.; Yi, J.; Ryu, D. Y. Oxidative Stress-Dependent Toxicity of Silver Nanoparticles in Human Hepatoma Cells. *Toxicol. In Vitro* **2009**, *23*, 1076−1084.

(12) Garza-Ocanas, L.; Ramirez-Cabrera, M.; Zanatta-Calderon, M. T.; Lujan-Rangel, R.; Ferrer, D. A.; Yacaman, M. J. In Vitro Toxicity Assessment of Silver Nanoparticles in Chang Liver Cells and J-774 Macrophages. *Toxicol. Lett.* **2010**, *196*, S284−S284.

(13) Sung, J. H.; Ji, J. H.; Song, K. S.; Lee, J. H.; Choi, K. H.; Lee, S. H.; Yu, I. J. Acute Inhalation Toxicity of Silver Nanoparticles. *Toxicol. Ind. Health* **2011**, *27*, 149−154.

(14) Ji, J. H.; Yu, I. J. Estimation of Human Equivalent Exposure from Rat Inhalation Toxicity Study of Silver Nanoparticles Using Multi-Path Particle Dosimetry Model. *Toxicol. Res.* **2012**, *1*, 206−210.

(15) van der Zande, M.; Vandebriel, R. J.; Van Doren, E.; Kramer, E.; Rivera, Z. H.; Serrano-Rojero, C. S.; Gremmer, E. R.; Mast, J.; Peters, R. J. B.; Hollman, P. C. H.; Hendriksen, P. J. M.; Marvin, H. J. P.; Peijnenburg, A. A. C. M.; Bouwmeester, H. Distribution, Elimination, and Toxicity of Silver Nanoparticles and Silver Ions in Rats after 28-Day Oral Exposure. *ACS Nano* **2012**, *6*, 7427−7442.

(16) Muth-Kohne, E.; Sonnack, L.; Schlich, K.; Hischen, F.; Baumgartner, W.; Hund-Rinke, K.; Schafers, C.; Fenske, M. The Toxicity of Silver Nanoparticles to Zebrafish Embryos Increases through Sewage Treatment Processes. *Ecotoxicology* **2013**, *22*, 1264−1277.

(17) Pratsinis, A.; Hervella, P.; Leroux, J. C.; Pratsinis, S. E.; Sotiriou, G. A. Toxicity of Silver Nanoparticles in Macrophages. *Small* **2013**, *9*, 2576−2584.

(18) Hadrup, N.; Lam, H. R. Oral Toxicity of Silver Ions, Silver Nanoparticles, and Colloidal Silver—A Review. *Regul. Toxicol. Pharmacol.* **2014**, *68*, 1−7.

(19) Ivask, A.; ElBadawy, A.; Kaweeteerawat, C.; Boren, D.; Fischer, H.; Ji, Z. X.; Chang, C. H.; Liu, R.; Tolaymat, T.; Telesca, D.; Zink, J. I.; Cohen, Y.; Holden, P. A.; Godwin, H. A. Toxicity Mechanisms in *Escherichia coli* Vary for Silver Nanoparticles and Differ from Ionic Silver. *ACS Nano* **2014**, *8*, 374−386.

(20) Ribeiro, F.; Gallego-Urrea, J. A.; Jurkschat, K.; Crossley, A.; Hassellov, M.; Taylor, C.; Soares, A. M. V. M; Loureiro, S. Silver Nanoparticles and Silver Nitrate Induce High Toxicity to *Pseudokirchneriella subcapitata*, *Daphnia magna* and *Danio rerio*. *Sci. Total Environ.* **2014**, *466*, 232−241.

(21) Wang, X.; Ji, Z. X.; Chang, C. H.; Zhang, H. Y.; Wang, M. Y.; Liao, Y. P.; Lin, S. J.; Meng, H.; Li, R. B.; Sun, B. B.; Winkle, L. V.; Pinkerton, K. E.; Zink, J. I.; Xia, T.; Nel, A. E. Use of Coated Silver Nanoparticles to Understand the Relationship of Particle Dissolution and Bioavailability to Cell and Lung Toxicological Potential. *Small* **2014**, *10*, 385−398.

(22) Bovenkamp, G. L.; Zanzen, U.; Krishna, K. S.; Hormes, J.; Prange, A. X-Ray Absorption near-Edge Structure (XANES) Spectroscopy Study of the Interaction of Silver Ions with *Staphylococcus aureus*, *Listeria monocytogenes*, and *Escherichia coli*. *Appl. Environ. Microbiol.* **2013**, *79*, 6385−6390.

(23) Jung, W. K.; Koo, H. C.; Kim, K. W.; Shin, S.; Kim, S. H.; Park, Y. H. Antibacterial Activity and Mechanism of Action of the Silver Ion in *Staphylococcus aureus* and *Escherichia coli*. *Appl. Environ. Microbiol.* **2008**, *74*, 2171−2178.

(24) Chopra, I. The Increasing Use of Silver-Based Products as Antimicrobial Agents: A Useful Development or a Cause for Concern? *J. Antimicrob. Chemother.* **2007**, *59*, 587−590.

(25) Eom, H. J.; Choi, J. Comparative Toxicity of Silver Nanoparticles and Silver Ions in Human Lymphoma Cell, Jurkat Using MRNA and MicroRNA Expression Profiling Analysis. *Mol. Cell. Toxicol.* **2009**, *5*, 82−82.

(26) Kittler, S.; Greulich, C.; Diendorf, J.; Koller, M.; Epple, M. Toxicity of Silver Nanoparticles Increases During Storage Because of Slow Dissolution under Release of Silver Ions. *Chem. Mater.* **2010**, *22*, 4548−4554.

(27) Beer, C.; Foldbjerg, R.; Dang, D. A.; Autrup, H. Genotoxicity and Toxicity of Silver Nanoparticles and Silver Ions. *Toxicol. Lett.* **2011**, *205*, S44−S44.

(28) Beer, C.; Foldbjerg, R.; Hayashi, Y.; Sutherland, D. S.; Autrup, H. Toxicity of Silver Nanoparticles—Nanoparticle or Silver Ion? *Toxicol. Lett.* **2012**, *208*, 286−292.

(29) Reidy, B.; Haase, A.; Luch, A.; Dawson, K. A.; Lynch, I. Mechanisms of Silver Nanoparticle Release, Transformation and Toxicity: A Critical Review of Current Knowledge and Recommendations for Future Studies and Applications. *Materials* **2013**, *6*, 2295−2350.

(30) Sackesen, C.; Ercan, H.; Dizdar, E.; Soyer, O.; Gumus, P.; Tosun, B. N.; Buyuktuncer, Z.; Karabulut, E.; Besler, T.; Kalayci, O. A Comprehensive Evaluation of the Enzymatic and Nonenzymatic Antioxidant Systems in Childhood Asthma. *J. Allergy Clin. Immunol.* **2008**, *122*, 78−85.

(31) Li, N.; Sioutas, C.; Cho, A.; Schmitz, D.; Misra, C.; Sempf, J.; Wang, M. Y.; Oberley, T.; Froines, J.; Nel, A. Ultrafine Particulate Pollutants Induce Oxidative Stress and Mitochondrial Damage. *Environ. Health Perspect.* **2003**, *111*, 455−460.

(32) Chan, J. K. W.; Charrier, J. G.; Kodani, S. D.; Vogel, C. F.; Kado, S. Y.; Anderson, D. S.; Anastasio, C.; Van Winkle, L. S. Combustion-Derived Flame Generated Ultrafine Soot Generates Reactive Oxygen Species and Activates Nrf2 Antioxidants Differently in Neonatal and Adult Rat Lungs. *Part. Fibre Toxicol.* **2013**, *10* (34), 1−18.

(33) Levard, C.; Hotze, E. M.; Lowry, G. V.; Brown, G. E. Environmental Transformations of Silver Nanoparticles: Impact on Stability and Toxicity. *Environ. Sci. Technol.* **2012**, *46*, 6900−6914.

(34) Loza, K.; Diendorf, J.; Sengstock, C.; Ruiz-Gonzalez, L.; Gonzalez-Calbet, J. M.; Vallet-Regi, M.; Koller, M.; Epple, M. The Dissolution and Biological Effects of Silver Nanoparticles in Biological Media. *J. Mater. Chem. B* **2014**, *2*, 1634−1643.

DOI: 10.1021/jp510103m
J. Phys. Chem. A 2015, 119, 281−289

(35) Flory, J. R. *Influence of pH on the Transport of Silver Nanoparticles in Saturated Porous Media: Laboratory Experiments and Modeling*; Air Force Institute of Technology: Wright-Patterson Air Force Base, OH, 2012.
(36) Liu, J. Y.; Wang, Z. Y.; Liu, F. D.; Kane, A. B.; Hurt, R. H. Chemical Transformations of Nanosilver in Biological Environments. *ACS Nano* **2012**, *6*, 9887−9899.
(37) Marchiol, L.; Mattiello, A.; Poscic, F.; Giordano, C.; Musetti, R. In Vivo Synthesis of Nanomaterials in Plants: Location of Silver Nanoparticles and Plant Metabolism. *Nanoscale Res. Lett.* **2014**, *9* (101), 1−11.
(38) Glover, R. D.; Miller, J. M.; Hutchison, J. E. Generation of Metal Nanoparticles from Silver and Copper Objects: Nanoparticle Dynamics on Surfaces and Potential Sources of Nanoparticles in the Environment. *ACS Nano* **2011**, *5*, 8950−8957.
(39) Davidson, R. A.; Guo, T. An Example of X-Ray Nanochemistry: SERS Investigation of Polymerization Enhanced by Nanostructures under X-Ray Irradiation. *J. Phys. Chem. Lett.* **2012**, *3*, 3271−3275.
(40) Anderson, D. S.; Silva, R. G.; Lee, D.; Edwards, P. C.; Sharmah, A.; Guo, T.; Pinkerton, K. E.; Van Winkle, L. S. Persistence of Silver Nanoparticles in the Rat Lung: Influence of Dose, Size and Chemical Composition. *Nanotoxicology* **2014**, *18*, 1−12.
(41) Herzog, F.; Clift, M. J. D.; Piccapietra, F.; Behra, R.; Schmid, O.; Petri-Fink, A.; Rothen-Rutishauser, B. Exposure of Silver-Nanoparticles and Silver-Ions to Lung Cells in Vitro at the Air-Liquid Interface. *Part. Fibre Toxicol.* **2013**, *10* (11), 1−14.
(42) Quadros, M. E.; Pierson, R.; Tulve, N. S.; Willis, R.; Rogers, K.; Thomas, T. A.; Marr, L. C. Release of Silver from Nanotechnology-Based Consumer Products for Children. *Environ. Sci. Technol.* **2013**, *47*, 8894−8901.
(43) Fukuda, N.; Ishida, N.; Nomura, K.; Wang, T.; Tamada, K.; Ushijima, H. Analysis of Adsorption and Binding Behaviors of Silver Nanoparticles onto a Pyridyl-Terminated Surface Using XPS and AFM. *Langmuir* **2011**, *27*, 12916−12922.
(44) Asoro, M. A.; Kovar, D.; Ferreira, P. J. Effect of Surface Carbon Coating on Sintering of Silver Nanoparticles: In Situ Tem Observations. *Chem. Commun.* **2014**, *50*, 4835−4838.
(45) Ortega, R.; Carmona, A.; Llorens, I.; Solari, P. L. X-Ray Absorption Spectroscopy of Biological Samples. A Tutorial. *J. Anal. At. Spectrom.* **2012**, *27*, 2054−2065.
(46) Nishimura, S.; Mott, D.; Takagaki, A.; Maenosono, S.; Ebitani, K. Role of Base in the Formation of Silver Nanoparticles Synthesized Using Sodium Acrylate as a Dual Reducing and Encapsulating Agent. *Phys. Chem. Chem. Phys.* **2011**, *13*, 9335−9343.
(47) Blanton, T. N.; Whitcomb, D. R.; Misture, S. T. An EXAFS Study of Photographic Development in Thermographic Films. *Powder Diffr.* **2007**, *22*, 122−125.
(48) Doolette, C. L.; McLaughlin, M. J.; Kirby, J. K.; Batstone, D. J.; Harris, H. H.; Ge, H. Q.; Cornelis, G. Transformation of PVP Coated Silver Nanoparticles in a Simulated Wastewater Treatment Process and the Effect on Microbial Communities. *Chem. Cent. J.* **2013**, *7* (46), 1−18.
(49) Miyanaga, T.; Suzuki, Y.; Matsumoto, N.; Narita, S.; Ainai, T.; Hoshino, H. Formation of Ag Clusters in Zeolite X Studied by in Situ EXAFS and Infrared Spectroscopy. *Microporous Mesoporous Mater.* **2013**, *168*, 213−220.
(50) Padovani, S.; Puzzovio, D.; Sada, C.; Mazzoldi, P.; Borgia, I.; Sgamellotti, A.; Brunetti, B. G.; Cartechini, L.; D'acapito, F.; Maurizio, C.; Shokoui, F.; Oliaiy, P.; Rahighi, J.; Lamehi-Rachti, M.; Pantos, E. XAFS Study of Copper and Silver Nanoparticles in Glazes of Medieval Middle-East Lustreware (10th−13th Century). *Appl. Phys. A: Mater. Sci. Process.* **2006**, *83*, 521−528.
(51) Dubiel, M.; Brunsch, S.; Troger, L. Characterization of Nanoscale Silver Particles in Glasses by Temperature-Dependent EXAFS Spectroscopy. *J. Phys.: Condens. Matter* **2000**, *12*, 4775−4789.
(52) Perrault, S. D.; Chan, W. C. W. Synthesis and Surface Modification of Highly Monodispersed, Spherical Gold Nanoparticles of 50−200 nm. *J. Am. Chem. Soc.* **2009**, *131*, 17042−17403.
(53) Plech, A.; Kimling, J.; Maier, M.; Okenve, B.; Kotaidis, V.; Ballot, H. Turkevich Method for Gold Nanoparticle Synthesis Revisited. *J. Phys. Chem. B* **2006**, *110*, 15700−15707.
(54) Raabe, O. G.; Bennick, J. E.; Light, M. E.; Hobbs, C. H.; Thomas, R. L.; Tillery, M. I. Improved Apparatus for Acute Inhalation Exposure of Rodents to Radioactive Aerosols. *Toxicol. Appl. Pharmacol.* **1973**, *26*, 264−273.
(55) Anderson, D. S.; Patchin, E. S.; Silva, R. G.; Uyeminami, D. L.; Sharmah, A.; Guo, T.; Brown, J. M.; Shannanhan, J.; Gordon, T.; Chen, L. C.; Pinkerton, K. E.; Van Winkle, L. S. Influence of Particle Size on Persistence and Clearance of Aerosolized Silver Nanoparticles in the Rat Lung. *Part. Fibre Toxicol.* **2014**, Revision Submitted.
(56) Cheng, G.; Guo, T. Surface Segregation in Ni/Co Bimetallic Nanoparticles Produced in Single-Walled Carbon Nanotube Synthesis. *J. Phys. Chem. B* **2002**, *106*, 5833−5839.
(57) Koningsberger, D. C.; Prins, R. *X-Ray Absorption: Principles, Applications, Techniques of EXAFS, SEXAFS and XANES*; John Wiley & Sons: New York, 1988; Vol. *92*.
(58) Webb, S. M. Sixpack: A Graphical User Interface for XAS Analysis Using IFEFFIT. *Phys. Scr.* **2005**, *T115*, 1011−1014.
(59) Sarode, P. R.; Priolkar, K. R.; Bera, P.; Hegde, M. S.; Emura, S.; Kumashiro, R. Study of Local Environment of Ag in Ag/CeO_2 Catalyst by Exafs. *Mater. Res. Bull.* **2002**, *37*, 1679−1690.
(60) Benfield, R. E. Mean Coordination Numbers and the Non-Metal Metal Transition in Clusters. *J. Chem. Soc., Faraday Trans.* **1992**, *88*, 1107−1110.
(61) Jentys, A. Estimation of Mean Size and Shape of Small Metal Particles by Exafs. *Phys. Chem. Chem. Phys.* **1999**, *1*, 4059−4063.
(62) Nishimura, S.; Anh, T. N. D.; Mott, D.; Ebitani, K.; Maenosono, S. X-Ray Absorption near-Edge Structure and X-Ray Photoelectron Spectroscopy Studies of Interfacial Charge Transfer in Gold−Silver−Gold Double-Shell Nanoparticles. *J. Phys. Chem. C* **2012**, *116*, 4511−4516.

DOI: 10.1021/jp510103m
J. Phys. Chem. A 2015, 119, 281−289